The combination of targeted vaccination and ring vaccination

Cite as: Chaos **31**, 063108 (2021); https://doi.org/10.1063/5.0048457
Submitted: 23 February 2021 • Accepted: 19 May 2021 • Published Online: 07 June 2021

Weiqiang Li, Jin Zhou, Zhen Jin, et al.

The combination of targeted vaccination and ring vaccination

Cite as: Chaos **31**, 063108 (2021); doi: 10.1063/5.0048457
Submitted: 23 February 2021 · Accepted: 19 May 2021 ·
Published Online: 7 June 2021

Weiqiang Li,[1] Jin Zhou,[1,a)] Zhen Jin,[2,3] and Jun-an Lu[1]

AFFILIATIONS

[1]School of Mathematics and Statistics, Wuhan University, Wuhan 430072, China
[2]Complex Systems Research Center, Shanxi University, Taiyuan 030006, China
[3]Shanxi Key Laboratory of Mathematical Techniques and Big Data Analysis on Disease Control and Prevention, Shanxi University, Taiyuan 030006, China

[a)]**Author to whom correspondence should be addressed:** jzhou@whu.edu.cn

ABSTRACT

Complex networks have become an important tool for investigating epidemic dynamics. A widely concerned research field for epidemics is to develop and study mitigation strategies or control measures. In this paper, we devote our attention to ring vaccination and targeted vaccination and consider the combination of them. Based on the different roles ring vaccination plays in the mixed strategy, the whole parameter space can be roughly divided into two regimes. In one regime, the mixed strategy performs poorly compared with targeted vaccination alone, while in the other regime, the addition of ring vaccination can improve the performance of targeted vaccination. This result gives us the more general and overall comparison between targeted and ring vaccination. In addition, we construct a susceptible–infected–recovered epidemic model coupled with the immunization dynamics on random networks. The comparison between stochastic simulations and numerical simulations confirms the validity of the model we propose.

To develop and study mitigation strategies and control measures for an epidemic is an important research field of epidemic dynamics. Until now, a lot of mechanisms have been investigated. However, every method has its own advantages and shortcomings. Given this fact, in this paper, we consider the combination of two kinds of immunization strategies: targeted vaccination and ring vaccination. The results show that, located in the different regions of parameter space, ring vaccination plays two distinct roles in the mixed immunization strategy. In addition, the comparison between stochastic simulations and numerical solutions confirms the validity of the model we propose.

I. INTRODUCTION

Complex networks have become an important tool for investigating epidemic dynamics.[1] The introduction of complex networks gives rise to a series of important issues such as the modeling of epidemic dynamics on complex networks and the studying of evolution spreading in complex networks.[2,3] Moreover, to develop and study mitigation strategies and control measures for epidemics is also a focus of research.[4] Although some achievements have been attained, a lot of work remains to be proceeding.

In this paper, we focus our attention on immunization strategy. As summarized in Refs. 4 and 5, some early mechanisms in the literature mainly include random vaccination,[6] targeted vaccination,[6] and acquaintance vaccination.[7] All the three possess one common characteristic: the immunization process has been conducted before the outbreak of disease. So, this type of immunization strategy can also be referred to as static immunization. On the other hand, several novel immunization schemes have been investigated in recent decades. Ruan *et al.* proposed an information-driven vaccination strategy.[8] Whether one susceptible individual receives a vaccine or not depends on the information collected from the neighbors. Another scheme, called contact immunization by Wu *et al.*, is aimed at a certain set of individuals, not all individuals, of the population, who get vaccinated with a rate if contacting at least one infected neighbor.[9] Furthermore, some authors introduced the observer nodes as the warning roles. Once any neighbor of an observer is infected, the observer will inform the other neighbors

of taking the immunization measure.[10] To distinguish from static immunization described above, we call these strategies as dynamic immunization collectively.

At the same time, another method, named *ring vaccination*, received the researchers' attention long ago because of its wide applicability to some real diseases.[11,12] One advantage of ring vaccination is that the susceptible individuals in contact with at least one infected neighbor are the targets of ring vaccination, and, once immunized successfully, those individuals can thus directly block the transmission of the disease.[5,13] The actual performance of ring vaccination is, however, influenced by many factors. For example, the newly infected individuals are not usually been identified in time, and, as a result, the susceptible neighbors are likely to be infected before immunization.[12] By comparison, although there are a lot of shortcomings, static immunization has its own advantage. For instance, the implementation of static vaccination does not need to know the states of nodes. Alvarez-Zuzek *et al.* compared the performance of targeted vaccination with the one of ring vaccination on partially overlapped multiplex network.[5] In this paper, we concentrate our attention on considering the combination of targeted and ring vaccination on a single random network, which has received little attention before. What we mainly care about is that does the mixed vaccination strategy exhibit better performance than one isolated vaccination strategy? The answer can tell us the more general and overall comparison results between targeted and ring vaccination, which has important practical significance for the formulation of the immunization strategy.

The remaining part is organized as follows. In Sec. II, we develop a system of ordinary differential equations for describing a susceptible–infected–recovered (SIR) epidemic model under the mixed immunization strategy on random networks. The details of stochastic simulations are presented in Sec. III. We show the main results of this paper in Sec. IV. Finally, we give our discussions in Sec. V.

II. MODEL

In this paper, we consider a susceptible–infected–recovered (SIR) epidemic model coupled with the immunization dynamics on random networks. The basic SIR dynamics is described as follows: the infectious individuals will infect their susceptible neighbors at a rate β; meanwhile, they may recover at a rate γ and then be immune to future infection. Here, we discuss two kinds of immunization strategies: targeted vaccination and ring vaccination. We denote by p the proportion of individuals with the largest degrees who are vaccinated initially, while we use q to denote the rate at which the susceptible neighbors of infected individuals get immunized.

First, let us consider the case of the fraction p of individuals being initially vaccinated. For a network with the degree distribution p_k and the minimum and maximum degrees k_{min} and k_{max}, this corresponds to a degree threshold $k_c \in [k_{min}, k_{max}]$ and a real number $\sigma_c \in (0, 1]$ such that

$$p = \sum_{k=k_c+1}^{k_{max}} p_k + \sigma_c p_{k_c}.$$

The "effective" network structure has changed after targeted vaccination, due to the partly individuals' immunization and, consequently, the failure of the partial edges emanating from them.[6,14] Then, the "new" degree distribution can be given by

$$p'_k = C\left[\sum_{l=k}^{k_c-1} p_l \binom{l}{k} (1-\phi)^k \phi^{l-k} + (1-\sigma_c) p_{k_c} \binom{k_c}{k} (1-\phi)^k \phi^{k_c-k}\right], \quad 0 \le k \le k_c,$$

where ϕ represents the probability that the any link will be connected with an immunized node, that is,

$$\phi = \frac{\sum_{k=k_c+1}^{k_{max}} k p_k + \sigma_c k_c p_{k_c}}{\sum_{k=k_{min}}^{k_{max}} k p_k},$$

and C is a normalization constant. Note that the minimum degree of the new network becomes 0. This is because one node will "lose" all its links if its neighbors happen to be the ones with large degrees.

Second, by means of the effective degree model proposed by Lindquist *et al.*,[15] the dynamics of a SIR-type epidemic under ring vaccination on the above new network can be described by a system of ordinary differential equations (ODEs). Let S_{si} (I_{si}) be the number of susceptible (infectious) nodes with s susceptible and i infectious neighbors. Then, one has

$$\begin{aligned}\dot{S}_{si} = &-\beta i S_{si} + \gamma[(i+1)S_{s,i+1} - iS_{si}] \\ &+ [(s+1)S_{s+1,i-1} - sS_{si}]\frac{\sum_{k=1}^{k_c}\sum_{j+l=k}\beta j l S_{jl}}{\sum_{k=1}^{k_c}\sum_{j+l=k} jS_{jl}} \\ &- qiS_{si} + [(s+1)S_{s+1,i} - sS_{si}]\frac{\sum_{k=1}^{k_c}\sum_{j+l=k} q j l S_{jl}}{\sum_{k=1}^{k_c}\sum_{j+l=k} jS_{jl}}, \end{aligned} \tag{1}$$

$$\begin{aligned}\dot{I}_{si} = &\beta i S_{si} - \gamma I_{si} + \gamma[(i+1)I_{s,i+1} - iI_{si}] \\ &+ [(s+1)I_{s+1,i-1} - sI_{si}]\frac{\sum_{k=1}^{k_c}\sum_{j+l=k}\beta l^2 S_{jl}}{\sum_{k=1}^{k_c}\sum_{j+l=k} jI_{jl}} \\ &+ [(s+1)I_{s+1,i} - sI_{si}]\frac{\sum_{k=1}^{k_c}\sum_{j+l=k} q l^2 S_{jl}}{\sum_{k=1}^{k_c}\sum_{j+l=k} jI_{jl}} \end{aligned} \tag{2}$$

for $\{(s,i) : 0 \le s+i \le k_c, 0 \le s, i \le k_c\}$. Here, the sign $\cdot$ represents the time derivative.

For the right-hand side of Eq. (1), the first term represents the decrease of S_{si} at rate βi due to the infection of susceptible nodes themselves since there are i infected neighbors, the second term describes the change of S_{si} because of the recovery of infected neighbors, and the third term accounts for the change of S_{si} caused by the infection of susceptible neighbors, which is proportional to the number $\sum_{k=1}^{k_c}\sum_{j+l=k}\beta j l S_{jl}$ of susceptible nodes as the neighbors of the newly infected nodes per time and the probability $sS_{si}/\sum_{k=1}^{k_c}\sum_{j+l=k} jS_{jl}$ ($(s+1)S_{s+1,i}/\sum_{k=1}^{k_c}\sum_{j+l=k} jS_{jl}$) with which those susceptible nodes belong to class S_{si} ($S_{s+1,i}$). According to the above analysis for the infection process, the last two terms, corresponding to ring vaccination, can be explained in the same way.

By the definition of S_{si} and I_{si}, the number of susceptible and infectious nodes are

$$S = \sum_{k=0}^{k_c} \sum_{j+l=k} S_{jl}$$

and

$$I = \sum_{k=0}^{k_c} \sum_{j+l=k} I_{jl},$$

respectively. Then, the dynamical evolution of the number R of recovered nodes can be given by

$$\dot{R} = \gamma I. \tag{3}$$

Considering the demographic processes, such as birth and death, are not taken into consideration, we further have

$$V = N - S - I - R,$$

where V represents the number of vaccinated nodes and N the size of the network. It should be noted that V is composed of two parts: pN based on targeted vaccination and $(1-p)N - S - I - R$ based on ring vaccination.

Finally, the initial conditions of Eqs. (1)–(3) are stated below.[16] At the beginning, it is assumed that a small fraction ε of nodes is infected in the network, not including the ones who have been immunized before. In view of the small value of ε, there is little probability that two infected nodes are connected to each other or that one susceptible node has two or more infected neighbors at $t = 0$. Thus, $I_{k0}(0) = \varepsilon N_k$, $k \geq 0$, and $S_{k-1,1}(0) + S_{k0}(0) = (1-\varepsilon)N_k$, $k > 0$; $S_{00}(0) = (1-\varepsilon)N_0$, where $N_k = p'_k(1-p)N$, $0 \leq k \leq k_c$. Furthermore, it is probability ε with which one susceptible node is linked to one infected node. Then, $S_{k-1,1}(0) = \varepsilon(1-\varepsilon)N_k$, $k > 0$. To sum up,

$$\begin{cases} I_{k0}(0) = \varepsilon p'_k(1-p)N, & 0 \leq k \leq k_c, \\ S_{k0}(0) = (1-\varepsilon)p'_k(1-p)N, & k = 0, \\ S_{k-1,1}(0) = \varepsilon(1-\varepsilon)p'_k(1-p)N, & 1 \leq k \leq k_c, \\ S_{k0}(0) = (1-\varepsilon)^2 p'_k(1-p)N, & 1 \leq k \leq k_c. \end{cases}$$

According to Refs. 6, 14, 15, and 17, we can derive the disease threshold condition for SIR epidemic model under the mixed immunization strategy. For the case of $\sigma_c = 1$, the disease threshold condition is determined by a parameter

$$\mathscr{R}_0 = \frac{\beta}{\beta + \gamma + q} \frac{\langle k^2 \rangle_c - \langle k \rangle_c}{\langle k \rangle_c} (1 - \phi),$$

where $\langle k \rangle_c$ and $\langle k^2 \rangle_c$ are the first and second moments of the original degree distribution p_k with the new cut-off $k_c - 1$, respectively. In other words, $\langle k \rangle_c = \sum_{k=k_{min}}^{k_c-1} k p_k$ and $\langle k^2 \rangle_c = \sum_{k=k_{min}}^{k_c-1} k^2 p_k$. See more derivation details in the Appendix.

If $\mathscr{R}_0 < 1$, the disease can only cause few outbreaks, whereas if $\mathscr{R}_0 > 1$, the disease first invades a fraction of the population and dies out eventually.

III. STOCHASTIC SIMULATIONS

Random networks used in this paper are generated based on the configuration model, also called Molloy–Reed algorithm, which is well-known and widely used to generate random networks with arbitrary degree distribution.[18,19]

In this paper, we consider two kinds of networks. The first shows the homogeneous contact pattern of a Poisson degree distribution,

$$p_k = C_1 \frac{\lambda^{k_1} e^{-\lambda}}{k_1!}, \quad 0 \leq k_1 \leq k^1_{max},$$

as the networks generated by ER or WS model do.[20,21] The second displays the heterogeneous contact structure,

$$p_k = C_2 k_2^{-\tau}, \quad 1 \leq k_2 \leq k^2_{max},$$

like the networks generated by BA model feature.[22] Here, k^1_{max} and k^2_{max} are the maximum degrees, and C_1 and C_2 are normalization constants.[23]

The event-driven algorithm developed by Kiss *et al.*,[1] originated from the Gillespie algorithm,[24] is introduced to simulate the transmission of the disease on random networks. To incorporate ring vaccination into epidemic dynamics, we need to add an immunization process to the original event-driven algorithm. For every infectious node, each susceptible neighbor may undergo one of two possible processes: infection and immunization, which depends on the ordering of three random numbers, all generated from the exponential distribution with the corresponding parameters.[1,25]

Before each simulation, we pick out a fraction p of nodes with the largest degrees from random networks and immunize them. Then, a fraction ε of nodes are chosen at random as the initial infectious seeds, except the ones immunized earlier, with the remaining susceptible.

In the following, unless otherwise specified, we set $k^1_{max} = k^2_{max} = 12$, $\lambda = 6$, and $\tau = 0.2$, which ensures that two classes of generated networks have the same average degree $\langle k \rangle \simeq 6$. In addition, $N = 10^4$, $\gamma = 1.0$, and $\varepsilon = 10^{-3}$.

IV. RESULTS

In this section, we first give the comparison results of targeted vaccination and ring vaccination. Next, we further investigate the performance of the mixed immunization strategy.

Figure 1 shows the comparison between stochastic simulations and numerical simulations of Eqs. (1)–(3). From Fig. 1, we find that when β is relatively small, the size R of infection on the Power-law network is larger than that on the Poisson network; once β increases over some certain value, a reverse result is observed. A similar phenomenon has been revealed for epidemic dynamics without the immunization process.[23] Furthermore, as shown in Fig. 1(e), for ring vaccination, there exists a peak of the final fraction V of vaccinated individuals along increasing β, i.e., as β increases, the final fraction V of vaccinated individuals first increases until reaching the peak and then decreases, which can be attributed to the competition of two processes: transmission and immunization.[5] When β is large, the individuals under the risk of infection are more likely to be infected before vaccination, which leads to a decrease in the

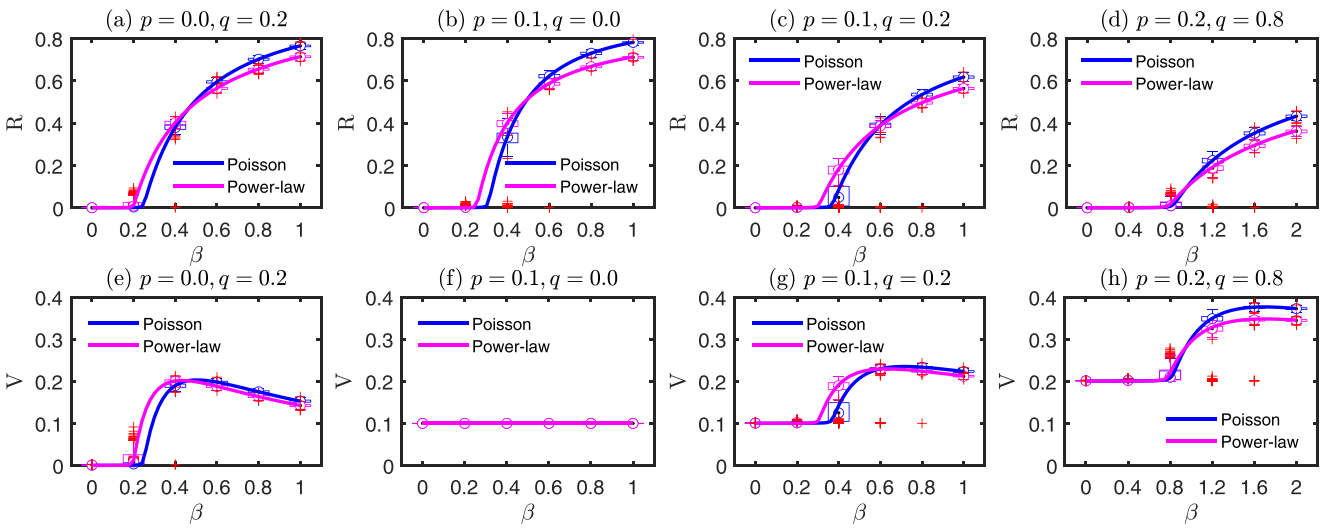

FIG. 1. The final fractions of recovered individuals R and vaccinated individuals V as a function of infection rate β under several combinations of targeted vaccination and ring vaccination. The blue (dark gray) and magenta (light gray) lines represent the numerical solutions of Eqs. (1)–(3) on the Poisson and Power-law networks, respectively. Each box plot corresponds to 500 results of stochastic simulation for a certain value of β, 50 independent runs on each of 10 networks, where the black dot inside a circle denotes the median of the simulation results and the outliers are plotted individually using the "+" symbol. (a) and (e) $p = 0.0, q = 0.2$; (b) and (f) $p = 0.1, q = 0.0$; (c) and (g) $p = 0.1, q = 0.2$; (d) and (h) $p = 0.2, q = 0.8$.

number of vaccinated individuals. Compared with low values of p and q, high values of p and q correspond to the smaller final epidemic size R and the higher critical infection rate β_c, above which an epidemic occurs, for both types of networks. In addition, except for several values close to the critical value β_c, we can see that the numerical solutions agree well with the simulation results for all the other values of β, which confirms the validity of the model we develop.

In Fig. 2, we compare ring vaccination with targeted vaccination. It can be seen from Fig. 2 that, for ring vaccination, when the rate q increases over a certain value and becomes more and more high, fewer individuals are vaccinated while fewer individuals are infected. This result is predictable since ring vaccination is aimed at the susceptible individuals connected with at least one infected neighbor, which determines that, for high rate q, ring vaccination can heavily block the spreading of disease. However, it is impossible for targeted vaccination: the smaller the final size R of the epidemic, the larger the initial fraction V of vaccinated individuals. On the other hand, there exists a critical size of the epidemic, denoted by R_c^s and R_c^w for the Poisson and Power-law networks, respectively. When the final sizes of the epidemic under two kinds of vaccination strategies, respectively, exceed this critical size, targeted vaccination performs better than ring vaccination, i.e., if the same epidemic sizes are obtained under two types of vaccination strategies respectively, fewer individuals are vaccinated based on targeted vaccination. Otherwise, the performance of ring vaccination is better than that of targeted vaccination. Moreover, Fig. 2 also indicates that, compared to the Poisson network, the higher critical rate q_c is needed in order to eradicate the disease on the Power-law network, particularly in the case of large β.

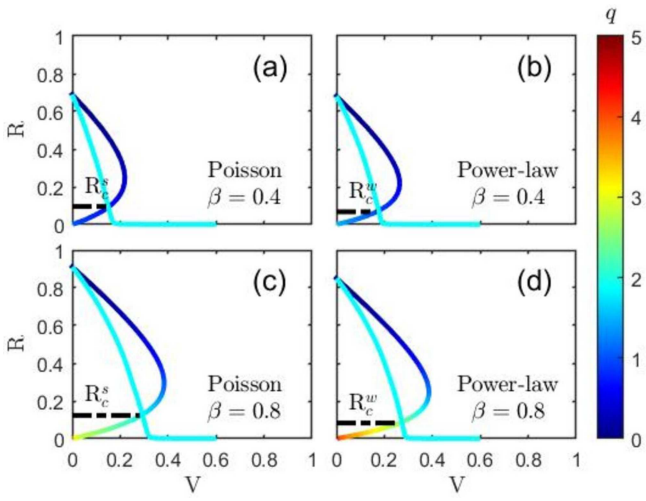

FIG. 2. The comparison between targeted vaccination and ring vaccination. The panels show the final sizes R of the epidemic vs the final fractions V of vaccinated individuals under different values of q and, as a contrast, the final fractions R of recovered individuals as a function of the initial fraction p/V of vaccinated individuals in four cases: (a) the Poisson network and $\beta = 0.4$; (b) the Power-law network and $\beta = 0.4$; (c) the Poisson network and $\beta = 0.8$; and (d) the Power-law network and $\beta = 0.8$, respectively. The cyan (light gray) lines correspond to targeted vaccination and the colored (graduated gray) ones ring vaccination. All values of q are mapped into the colormap. In each panel, under certain values of p and q, the final sizes R of the epidemic, denoted by R_c^s and R_c^w for the Poisson and Power-law networks, respectively, are the same as well as the final fractions V of vaccinated individuals.

Next, we consider the epidemic dynamics with the mixed immunization process. Figure 3 depicts the final fractions of recovered individuals R and vaccinated individuals V with respect to the whole population under various combinations of targeted vaccination and ring vaccination for $\beta = 0.8$, respectively. According to the findings in Fig. 2, the entire parameter space can be divided into two regimes: I and II, where the partition lines, the black solid lines in Fig. 3, capture the cases of the final epidemic sizes R being the critical values R_c^s and R_c^w for the Poisson and Power-law networks under different choices of the mixed strategy, respectively. To explore the roles ring vaccination plays in the mixed strategy in regime I and II, respectively, taking the case of the Power-law network as an example, we show two example cases of $R \simeq 0.5$ and $R \simeq 0.05$ in Fig. 4. From Fig. 4, we can see that, for all possible choices of the mixed strategy, under which the final sizes of the epidemic are approximately equal to 0.5, the red dashed lines in Figs. 3(c) and 3(d), the choice with a higher rate q of ring vaccination brings about a larger proportion V of vaccinated individuals; conversely, for the case of $R \simeq 0.05$, the blue dotted lines in Figs. 3(c) and 3(d), the choice with a higher rate q corresponds to a smaller fraction V. The above-mentioned statements are also applicable to the case of $\beta = 0.4$.

In addition, we also present two examples approaching R_c^w, one from the left and the other from the right in Fig. 4. One interesting

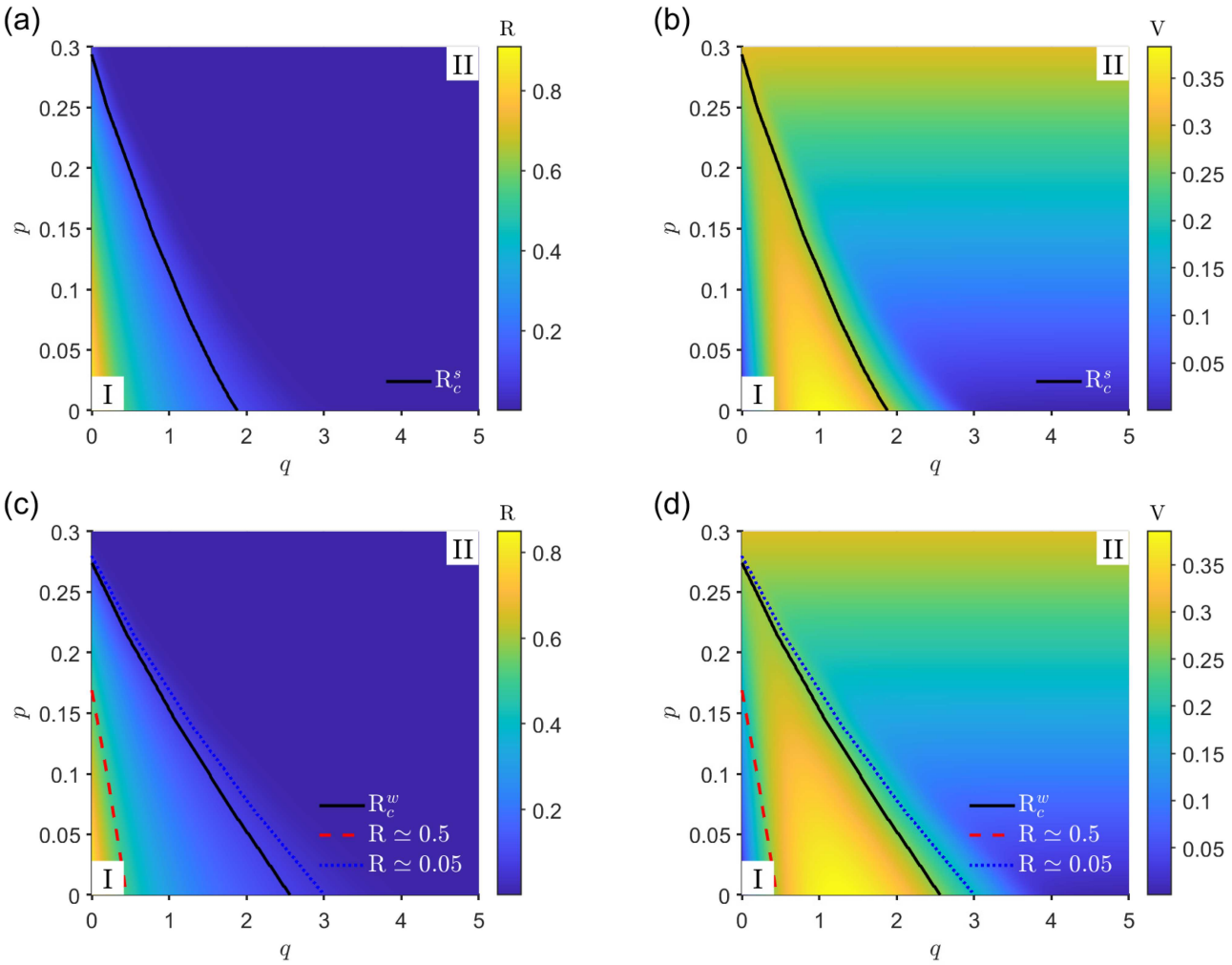

FIG. 3. The performance of the mixed immunization strategy. The final fractions of recovered individuals R and vaccinated individuals V are plotted as a function of p and q for $\beta = 0.8$, respectively. Panels (a) and (b) represent the case of the Poisson network, and panels (c) and (d) the case of the Power-law network. Corresponding to the case of the final fractions of recovered individuals being the critical value $R_c^s \simeq 0.130$ (the Poisson network) or $R_c^w \simeq 0.090$ (the Power-law network) under various choices of p and q, the black solid lines divide the whole parameter space into two regimes: I and II. The red dashed and blue dotted lines in the bottom panels show the case of the final epidemic sizes being 0.5 and 0.05, one above R_c^w and the other below R_c^w, respectively.

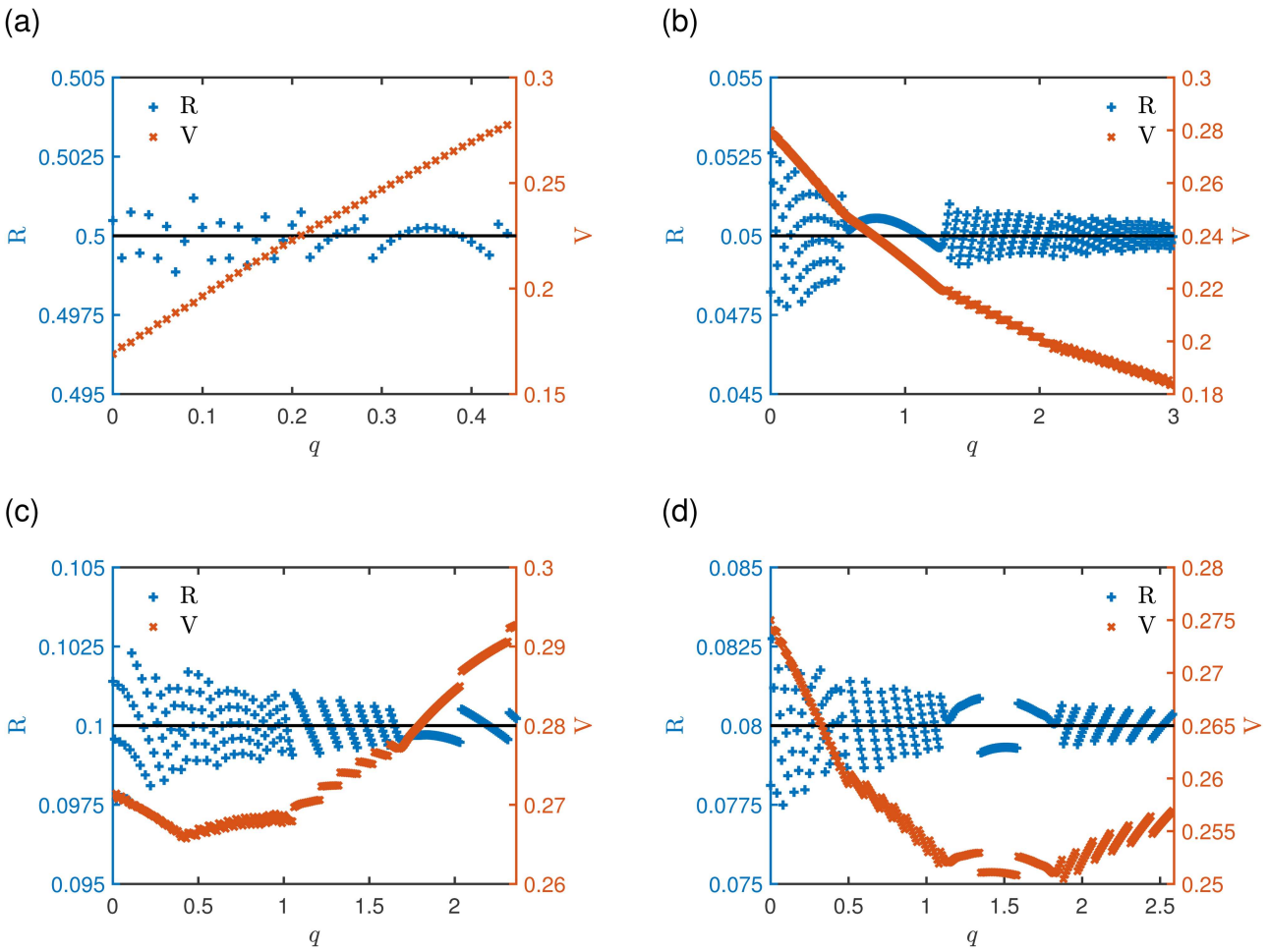

FIG. 4. The four examples for interpreting the difference between regime I and II shown in Fig. 3. The final sizes R of the epidemic and final fractions V of vaccinated individuals are plotted against the left and right y-axes under different choices of p and q, respectively, where each choice is chosen such that the final size R of the epidemic is close to one target value. In this figure, four target values are discussed: (a) 0.50, (b) 0.05, (c) 0.100, and (d) 0.080.

phenomenon appears: in both cases, with the rate q increasing in the mixed strategy, the final fraction V undergoes a change of falling first and then rising. One possible explanation for this is that, for targeted vaccination, compared with the nodes with large degrees, the immunization of the nodes with low degrees will be of less benefit. Therefore, when the mixed strategy approaches the critical case, a portion of targeted vaccination can be compensated by ring vaccination with an appropriate rate in a cost-effective way; however, ring vaccination cannot keep this advantage for a larger extent of the replacement of targeted vaccination.

V. DISCUSSION

In this paper, we have compared two kinds of immunization strategies: ring vaccination and targeted vaccination. The results show that only if the rate of ring vaccination is large enough is the performance of ring vaccination better than that of targeted vaccination. Further, we have investigated the performance of the mixed strategy. Based on the roles ring vaccination plays in the mixed strategy. The whole parameter space can be approximately divided into two regimes: in one regime, the mixed strategy performs poorly compared with targeted vaccination alone; in the other regime, the addition of ring vaccination can improve the performance of targeted vaccination.

The results obtained from this paper provide us with some guidance on the formulation of the immunization strategy when faced with a disease. As indicated in Figs. 3 and 4, for a disease, if the sick cannot be diagnosed or the neighbors of the sick cannot be recognized in time, which means a low rate of ring vaccination, targeted vaccination should be the prime option. However, once the

outbreak of disease can be governed below a certain critical level under the combination of targeted vaccination and ring vaccination, the importance of ring vaccination should be stressed, even in the case of a low rate of ring vaccination.

On the other hand, in realistic scenes, the implementation of ring vaccination and targeted vaccination is still confronted with a lot of challenges. For example, the accurate and quick recognition of the individuals with a large number of neighbors and with the infectious neighbors heavily determines the performance of targeted vaccination and ring vaccination, respectively. Furthermore, the individuals' or population's vaccination behavior is often influenced by other dynamics.[4] How to understand the interaction between vaccination behavior with other behaviors, such as adaptive and collective behaviors,[26–28] remains to be investigated.

ACKNOWLEDGMENTS

This work was supported by the National Natural Science Foundation of China (NNSFC) (Grant Nos. 61773294, 61773175, and 61873154) and the Fundamental Research Funds for the Central Universities.

APPENDIX: DERIVATION OF DISEASE THRESHOLD

Following the procedure in Ref. 15, we derive the disease threshold condition of the system of Eqs. (1) and (2) by studying the stability of the disease free equilibrium, i.e., $I_{si} = 0$ for all s and i; $S_{si} = 0$ for all $i \geq 1$, and $S_{s0} = N_s$ for all s.

To this end, we begin by introducing some approximations used below since, near the disease free equilibrium, the susceptible individuals with two or more infectious neighbors are rare, which implies that

$$\frac{\sum_{k=1}^{k_c}\sum_{j+l=k}\beta l^2 S_{jl}}{\sum_{k=1}^{k_c}\sum_{j+l=k} jI_{jl}} \approx \frac{\sum_{j=0}^{k_c-1}\beta S_{j1}}{\sum_{j=0}^{k_c-1} S_{j1}} = \beta \tag{A1}$$

and, similarly,

$$\frac{\sum_{k=1}^{k_c}\sum_{j+l=k} q l^2 S_{jl}}{\sum_{k=1}^{k_c}\sum_{j+l=k} jI_{jl}} \approx q, \tag{A2}$$

where we have used the balance equality $\sum_{k=1}^{k_c}\sum_{j+l=k} jI_{jl} = \sum_{k=1}^{k_c}\sum_{j+l=k} lS_{jl}$. Substituting the expressions (A1) and (A2) into Eq. (2), one thus has

$$\begin{aligned}\dot{I}_{si} = {} & \beta i S_{si} - \gamma I_{si} + \gamma[(i+1)I_{s,i+1} - iI_{si}] \\ & + \beta[(s+1)I_{s+1,i-1} - sI_{si}] + q[(s+1)I_{s+1,i} - sI_{si}]\end{aligned} \tag{A3}$$

near the disease free equilibrium.

Next, we calculate the Jacobian matrix, written as $\boldsymbol{F} - \boldsymbol{V}$, at the disease free equilibrium with respect to Eqs. (1) and (A3), where the matrix $\boldsymbol{F}$ involves the terms of transferring from class S_{s0} to class $S_{s-1,1}$ and the matrix $-\boldsymbol{V}$ the remaining terms. Take variables S_{si} and I_{si} in the lexicographical order: S_{si} first and I_{si} later; a sequence of increasing k, i.e., I_{00}; S_{01}, I_{10}, I_{01}; …; $S_{k_c-1,1}$, …, I_{0k_c}. Here, variables S_{k0}, $k \geq 0$, are not included because S_{k0} does not appear at any equation except that of $\dot{S}_{k0}$. Then, matrix $\boldsymbol{F}$ can be written as

$$\boldsymbol{F} = \frac{\beta}{\sum_{k=1}^{k_c} kN_k}\begin{bmatrix} u_0 \\ u_1 \\ \vdots \\ u_{k_c}\end{bmatrix}\left[v_0^T, v_1^T, \ldots, v_{k_c}^T\right], \tag{A4}$$

where u_k, $k = 1, \ldots, k_c$, are the $(2k+1) \times 1$ vectors with kN_k in the first entry and zero elsewhere, v_k, $k = 1, \ldots, k_c$, are the $(2k+1) \times 1$ vectors with $(k-1), 2(k-2), \ldots, s(k-s), \ldots, (k-1)$ in the first $(k-1)$ entries and zero elsewhere, and $u_0 = v_0 = 0$. Matrix $\boldsymbol{V}$ is block upper triangular, where except diagonal blocks V_{ii}, $i = 0, \ldots, k_c$, each lower triangular, and superdiagonal blocks $V_{i,i+1}$, $i = 0, \ldots, k_c - 1$, all other blocks are zero matrices. Notice also that all the entries of $\boldsymbol{V}$ are nonpositive except positive diagonal ones. Based on these results, it can be easily verified that matrix $\boldsymbol{F}$ is non-negative and matrix $\boldsymbol{V}$ is a non-singular M-matrix.[29] By Theorem 2 in Ref. 17, for matrices $\boldsymbol{F}$ and $\boldsymbol{V}$ satisfying the foregoing conditions, one thus has

$$s(\boldsymbol{F} - \boldsymbol{V}) = 0 \Leftrightarrow \rho(\boldsymbol{F}\boldsymbol{V}^{-1}) = 1,$$

where $s(\cdot)$ and $\rho(\cdot)$ denote the spectral abscissa and spectral radius of a matrix, respectively, and $\boldsymbol{V}^{-1}$ represents the inverse matrix of $\boldsymbol{V}$. So, the problem is now translated into seeking $\rho(\boldsymbol{F}\boldsymbol{V}^{-1})$. Note that all the entries in the first column of $V_{i,i+1}$, $i = 0, \ldots, k_c - 1$, are zero and the first $(k-1)$ entries in the first column of V_{ii}, $i = 0, \ldots, k_c$, are zero except the first positive entry.

Finally, the disease threshold condition is determined by a parameter

$$\mathscr{R}_0 = \rho(\boldsymbol{F}\boldsymbol{V}^{-1}) = \frac{\beta}{\beta+\gamma+q}\frac{\sum_{k=1}^{k_c} k(k-1)p'_k}{\sum_{k=1}^{k_c} kp'_k}.$$

On the other hand, according to Refs. 6 and 14, for the case of $\sigma_c = 1$, we further know $\langle k' \rangle = \langle k \rangle_c(1-\phi)$ and $\langle k'^2 \rangle = \langle k^2 \rangle_c(1-\phi)^2 + \langle k \rangle_c \phi(1-\phi)$, where $\langle k \rangle_c$ and $\langle k^2 \rangle_c$ are the first and second moments of the original degree distribution p_k with the new cut-off $k_c - 1$, while $\langle k' \rangle$ and $\langle k'^2 \rangle$ are the first and second moments of the new degree distribution p'_k. That is, $\langle k \rangle_c = \sum_{k=k_{min}}^{k_c-1} kp_k$ and $\langle k' \rangle = \sum_{k=0}^{k_c-1} kp'_k$. Thus, we further have

$$\mathscr{R}_0 = \frac{\beta}{\beta+\gamma+q}\frac{\langle k^2 \rangle_c - \langle k \rangle_c}{\langle k \rangle_c}(1-\phi).$$

In particular, if we do not consider two kinds of immunization strategies, the above result reduces to a well-known one, i.e., Ref. 15,

$$\mathscr{R}_0 = \rho(\boldsymbol{F}\boldsymbol{V}^{-1}) = \frac{\beta}{\beta+\gamma}\frac{\sum_{k=k_{min}}^{k_{max}} k(k-1)p_k}{\sum_{k=k_{min}}^{k_{max}} kp_k}.$$

DATA AVAILABILITY

The data that support the findings of this study are available from the corresponding author upon reasonable request.

REFERENCES

[1] I. Z. Kiss, J. C. Miller, and P. L. Simon, *Mathematics of Epidemics on Networks: From Exact to Approximate Models* (Springer International Publishing, Gewerbestrasse, 2017).
[2] R. Pastor-Satorras, C. Castellano, P. Van Mieghem, and A. Vespignani, "Epidemic processes in complex networks," Rev. Mod. Phys. **87**, 925–979 (2015).
[3] W. Wang, Q.-H. Liu, J. Liang, Y. Hu, and T. Zhou, "Coevolution spreading in complex networks," Phys. Rep. **820**, 1–51 (2019).
[4] Z. Wang, C. T. Bauch, S. Bhattacharyya, A. d'Onofrio, P. Manfredi, M. Perc, N. Perra, M. Salathé, and D. Zhao, "Statistical physics of vaccination," Phys. Rep. **664**, 1–113 (2016).
[5] L. G. Alvarez-Zuzek, M. A. Di Muro, S. Havlin, and L. A. Braunstein, "Dynamic vaccination in partially overlapped multiplex network," Phys. Rev. E **99**, 012302 (2019).
[6] R. Pastor-Satorras and A. Vespignani, "Immunization of complex networks," Phys. Rev. E **65**, 036104 (2002).
[7] R. Cohen, S. Havlin, and D. ben-Avraham, "Efficient immunization strategies for computer networks and populations," Phys. Rev. Lett. **91**, 247901 (2003).
[8] Z. Ruan, M. Tang, and Z. Liu, "Epidemic spreading with information-driven vaccination," Phys. Rev. E **86**, 036117 (2012).
[9] Q. Wu, X. Fu, Z. Jin, and M. Small, "Influence of dynamic immunization on epidemic spreading in networks," Physica A **419**, 566–574 (2015).
[10] Z. Li, P. Zhu, D. Zhao, Z. Deng, and Z. Wang, "Suppression of epidemic spreading process on multiplex networks via active immunization," Chaos **29**, 073111 (2019).
[11] J. Müller, B. Schönfisch, and M. Kirkilionis, "Ring vaccination," J. Math. Biol. **41**, 143–171 (2000).
[12] M. Kretzschmar, S. van den Hof, J. Wallinga, and J. van Wijngaarden, "Ring vaccination and smallpox control," Emerg. Infect. Dis. **10**, 832–841 (2004).
[13] M. A. Di Muro, L. G. Alvarez-Zuzek, S. Havlin, and L. A. Braunstein, "Multiple outbreaks in epidemic spreading with local vaccination and limited vaccines," New J. Phys. **20**, 083025 (2018).
[14] R. Cohen, K. Erez, D. Ben-Avraham, and S. Havlin, "Resilience of the internet to random breakdowns," Phys. Rev. Lett. **85**, 4626 (2000).
[15] J. Lindquist, J. Ma, P. van der Driessche, and F. H. Willeboordse, "Effective degree network disease models," J. Math. Biol. **62**, 143–164 (2011).
[16] E. Volz, "SIR dynamics on random networks with heterogeneous connectivity," J. Math. Biol. **56**, 293–310 (2008).
[17] P. van der Driessche and J. Watmough, "Reproduction numbers and subthreshold endemic equilibria for compartmental models of disease transmission," Math. Biosci. **180**, 29–48 (2002).
[18] M. Molloy and B. Reed, "A critical point for random graphs with a given degree sequence," Random Struct. Alg. **6**, 161–179 (1995).
[19] M. E. J. Newman, S. H. Strogatz, and D. J. Watts, "Random graphs with arbitrary degree distributions and their applications," Phys. Rev. E **64**, 026118 (2001).
[20] P. Erdős and A. Rényi, "On the evolution of random graphs," Publ. Math. Inst. Hung. Acad. Sci. **5**, 17–61 (1960).
[21] D. J. Watts and S. H. Strogatz, "Collective dynamics of 'small-world' networks," Nature **393**, 440–442 (1998).
[22] A.-L. Barabási and R. Albert, "Emergence of scaling in random networks," Science **286**, 509–512 (1999).
[23] V. Marceau, P.-A. Noël, L. Hébert-Dufresne, A. Allard, and L. J. Dubé, "Modeling the dynamical interaction between epidemics on overlay networks," Phys. Rev. E **84**, 026105 (2011).
[24] D. T. Gillespie, "Exact stochastic simulation of coupled chemical reactions," J. Phys. Chem. **81**, 2340–2361 (1977).
[25] M. Y. Li, *An Introduction to Mathematical Modeling of Infectious Diseases* (Springer International Publishing, Gewerbestrasse, 2018).
[26] X.-L. Peng, X.-J. Xu, M. Small, X. Fu, and Z. Jin, "Prevention of infectious diseases by public vaccination and individual protection," J. Math. Biol. **73**, 1561–1594 (2016).
[27] J. Zhou, J. Chen, J. Lu, and J. Lü, "On applicability of auxiliary system approach to detect generalized synchronization in complex network," IEEE Trans. Autom. Control **62**, 3468–3473 (2017).
[28] S. Zhu, J. Zhou, G. Chen, and J. Lu, "Estimating the region of attraction on a complex dynamical network," SIAM J. Control Optim. **57**, 1189–1208 (2019).
[29] A. Berman and R. J. Plemmons, *Nonnegative Matrices in the Mathematical Sciences* (Academic Press, New York, 1979).